1

# Application of IR Thermography for Studying Deformation and Fracture of Paper

Tatsuo Yamauchi
*Kyoto University*
*Japan*

## 1. Introduction

The deformation and fracture of paper have long been investigated from various points of view using many methods. Phenomena such as sound emission and thermal change occurring with the deformation have also been examined. Paper is a planar material and its thermal conductivity is low and further its specific heat is high; thus, the thermal change shown in surface temperature using IR thermography can be investigated related to the mechanical behavior. Advanced thermography with extensive computer memory and various imaging processes enables us to investigate the process of the deformation and fracture of paper. In this paper, studies on the fundamental thermodynamics of paper material are first critically introduced, discussing the effects of defects and unevenness of paper formation. Secondly, uneven thermal distribution and its time-sequential changes during the fracture toughness testing of paper are presented; that is to say, stress concentration and crack development at the notch tip which occurred during the deformation of paper with a notch could be visualized as serial images using IR thermography. The results helped to develop fracture toughness testing of paper and further gave an understanding of the fracture toughness of paper itself.

## 2. Application of thermography to investigate material deformation

The deforming and fracturing processes of solid material under stress are directly related to its mechanical strength, and thus are very important for many of its practical uses. A great number of studies relating to deforming and fracturing processes have been made from both experimental and theoretical points of view. Regarding paper material, a representative of two-dimensional planar material, its tensile load / elongation behavior has exclusively been investigated (Seth and Page, 1981; Chao and Sutton, 1988; Yamauchi et al., 1990). Among those studies thermodynamics of deformation is one of the basic subjects. Studying the fracture mechanisms of solid material from the viewpoint of thermodynamics has been proposed for a long time (Muller,1969). It is well known that the deformation process of solid material accompanies the generation and absorption of heat; however, it is not easy to measure the heat change or the change of the temperature of solid material under deformation and the related knowledge is still fragmentary even at the present time. In these circumstances, the measurement of infrared ray radiation from material is fairly popular as a non—contact method to measure temperature. This method started as a point

measurement, progressed to a line measurement and further developed to measure a series of sequential two-dimensional temperature images for a material surface, that is, modern infrared thermography. Thus, the overall surface temperature was experimentally obtained without any difficulty; however, it did not assign the internal temperature of the three-dimensional material to study the thermodynamics. This gap between the surface and interior is one reason why the thermodynamics of solid deformation has been little studied. The surface temperature of two-dimensional planar material could be regarded as the real temperature of the material, as experimentally shown later (referring to the last paragraph of **6**. Effect of paper formation, see Fig. 12).; therefore, thermography was applied to observe the deformation of paper materials ( Yamauchi et al., 1993).

From a technical point of view, the advancements of IR sensing, image processing with help of computer enabled a commercially available thermography measurement system equipped with high sensitive temperature detection of 0.1℃, image subtraction among serial images, histogram processing, mean value calculating functions and so on. This modern thermography measurement system was first commercialized for medical uses especially for breast cancer detection, and has since been used for non-destructive testing (NDT) of heating systems and quality inspection in commercial manufacturing. These are almost all static uses and dynamic use was limited, excluding the use of a special equipment combined with thermography to determine stress distribution within a solid material under strain (Koizumi, 1983). Thus, using this commercially available equipment named a stress analyser, imaginary calculation was conducted using temperature image changes caused by periodically given ultra-low distortion. The first trial of the dynamic use of thermography to display temperature images was probably conducted to detect fatigue-related heat emission in composite materials (Reifsnider and Williams, 1974).; however, first-stage thermography could not produce successive images to show the deformation process. A full—scale study of the deformation process was then conducted using advanced modern thermography for paper material (Yamauchi et al., 1993), partly because the thermal conductivity of which is low and thus suitable for consecutive observation of temperature images.

## 3. Temperature (heat) change during the tensile deformation of paper

Heat generation and absorption occurring during the tensile deformation process of paper was investigated with an in-house developed micro-calorimeter attached with straining device (Ebeling et al., 1974) by Ebeling. Figure 1 gives a representative result showing the heat absorption firstly occurred in the elastic tensile deformation region and heat generation caused by further straining in the plastic deformation region (Ebeling, 1976). He concluded that the heat absorption was caused by Kelvin's thermoelastic effect (heat generation in compression mode) and heat generation in the plastic deformation region was mainly due to irreversible deformation of fibers. At the same time, heat generation and adsorption occurring during the tensile deformation of paper were investigated with an infra-red line scanner (Dumbleton et al., 1973). This method also detected the initial cooling of paper specimens during elastic extension as well as the temperature rise due to energy dissipation during plastic deformation, as shown in Fig. 2. It was further found that energy change occurred throughout the specimen in a fairly uniform manner up to the moment of rupture, at which time the temperature increased instantaneously throughout the specimen and it was possible to account for from 40 to 80 % of the mechanical energy losses as increases in thermal energy.

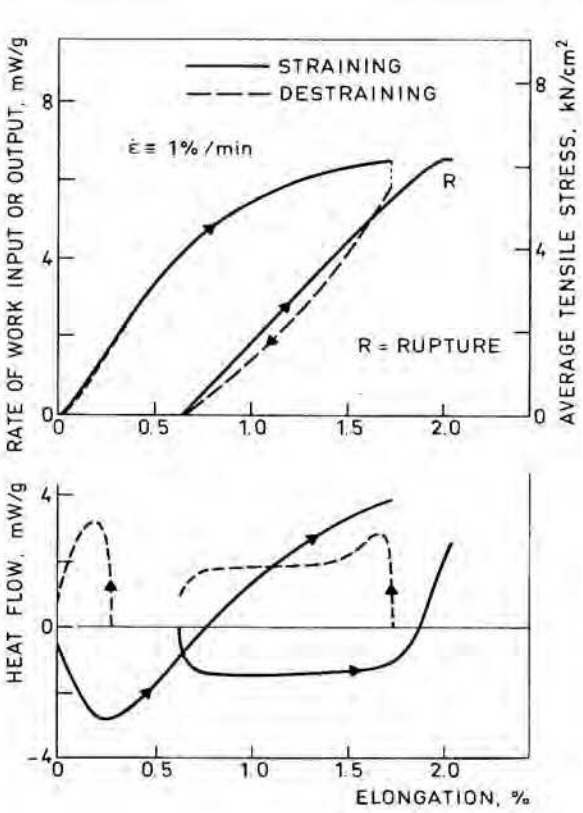


Fig. 1. Thermodynamic behavior of paper on tensile loading (Ebeling, 1976).

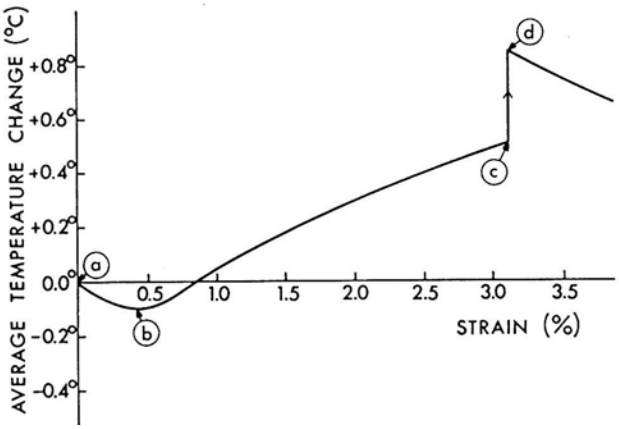


Fig. 2. Integrated average thermal response of paper on tensile loading (Dumbleton et al., 1973).

As to the temperature determination based on infrared radiation, the emissivity of paper is indispensable. Although it is considered to be about 0.9, 1.0 has been used for a long time as a perfect black body (Yamauchi et al., 1993), partly because of experimental difficulty in the determination. On the other hand, taking advantage of thermal emissivity difference in part, thermograph is applicable to measure moisture distribution and water absorption behavior of paper (Vickery et al., 1978; Tajima et al., 2011).

## 4. Application of thermography to study the tensile deforming process of paper

As shown in Fig. 3, the tensile behavior of paper was experimentally determined as the load–elongation relation and sequential surface temperature images of paper during tensile loading were spontaneously observed (Fig, 4) using modern thermography, and then the average temperature and histogram display of the temperature distribution were calculated (Fig. 5) (Yamauchi et al., 1993). Furthermore, a change in the average temperature during loading and the corresponding load—elongation curve were obtained, as shown in Fig. 6. Although the sensor sensitivity is 0.1℃ and the temperature change is very slight, averaging many temperature pixels caused a marked improvement of the S/N ratio using modern thermography, and thus it was measured with extremely high precision. The result is quite similar to those determined using the calorimeter and the infra-red line scanner, the thermal energy and mechanical rupture energy ratio being 57% within a predictive range (Ebeling, 1976; Dumbleton, 1973).

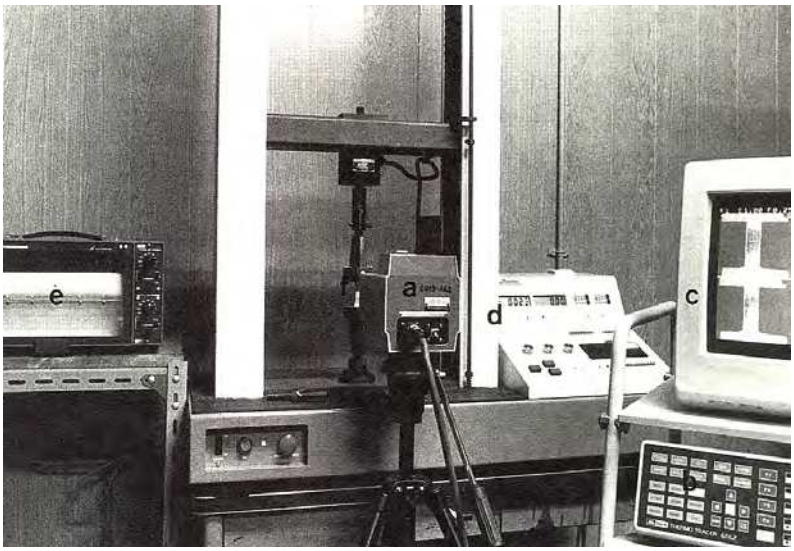


Fig. 3. Setup view of thermography for measuring the surface temperature of paper specimen under tensile strain: (a) infrared camera; (b) control unit; (c) monitor display; (d) Instron-type machine; (e) recorder; (f) paper specimen (Yamauchi and Tanaka, 1994).

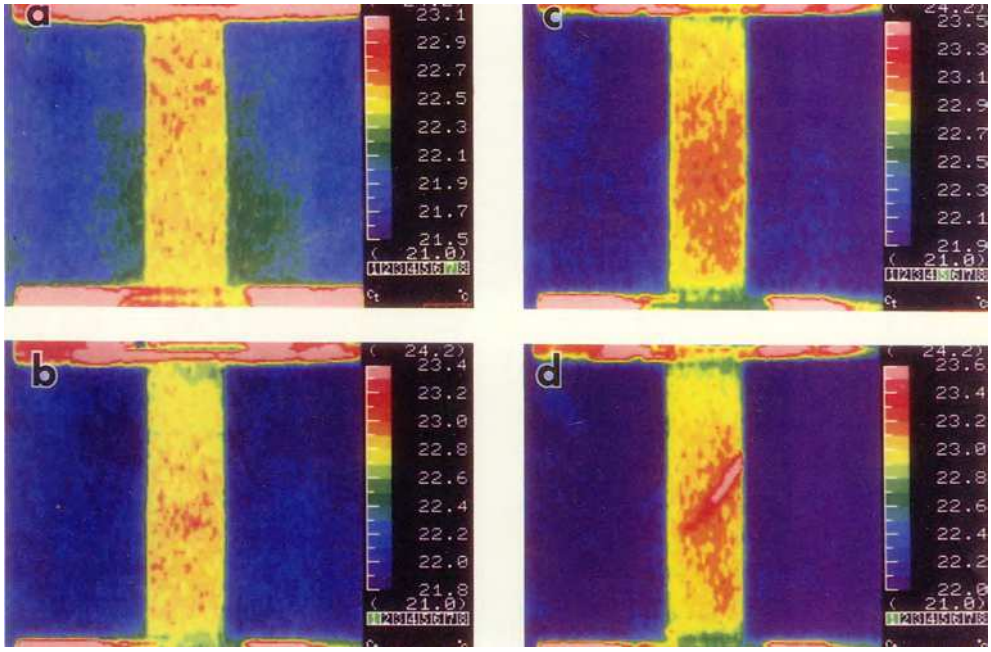


Fig. 4. A series of surface temperature images of paper under tensile strain. (a)-(d) correspond to the positions on the load-elongation curve in Fig. 6 (Yamauchi et al., 1993).

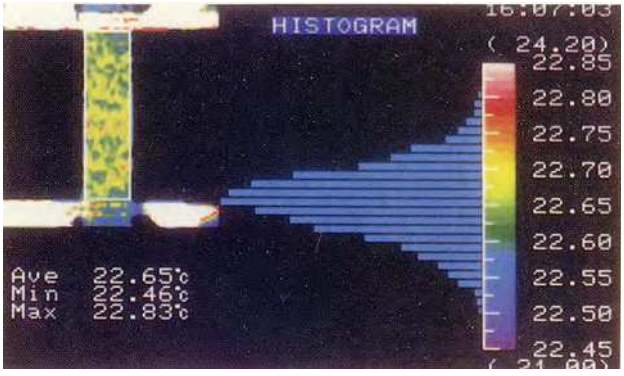


Fig. 5. Temperature image of paper under strain, histogram display of its temperature distribution, and calculated average temperature (Yamauchi et al., 1993).

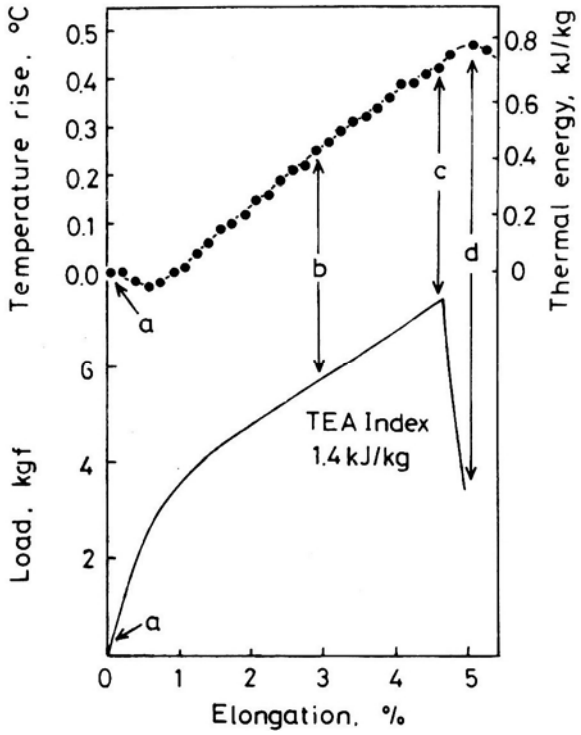


Fig. 6. Change of average temperature of paper under strain and the corresponding load-elongation curve (Yamauchi et al., 1993).

## 5. Thermal behavior of paper due to elastic elasticity and entropy elasticity

The initial tensile loading of paper accompanied cooling, which was in accordance with Kelvin's thermoelastic theory based on elastic elasticity. On the other hand, the heating of paper during plastic region elongation was interpreted as irreversible fiber deformation and the role of entropy elasticity was rejected, partly because of heat generation during unloading (Ebeling, 1976), although the mechanism of paper heating is still not clear. Subsequently, the thermal behavior of paper and rubber during unloading after highly tensile loading and ample successive stress-relaxation periods was examined in order to confirm this interpretation. Thus, a paper specimen was first strained up to about 80% of the breaking load, followed by being held at constant elongation for 1 h (stress-relaxation period) and then was destrained to zero load within 6 s (Yamauchi and Tanaka, 1994). The changes of load and the average temperature of the specimen during the above-mentioned process are shown in Fig. 7. Following the start of the tensile test, the temperature began to fall and reached a minimum at a point somewhat after the end point of the elastic deformation region. The temperature then rose almost linearly in the plastic deformation region. These behaviors are essentially the same as those described above. During the period of stress relaxation, the temperature becomes the surrounding temperature; that is to say, a period of 1h may be long enough to reach a temperature equilibrium. On destraining,

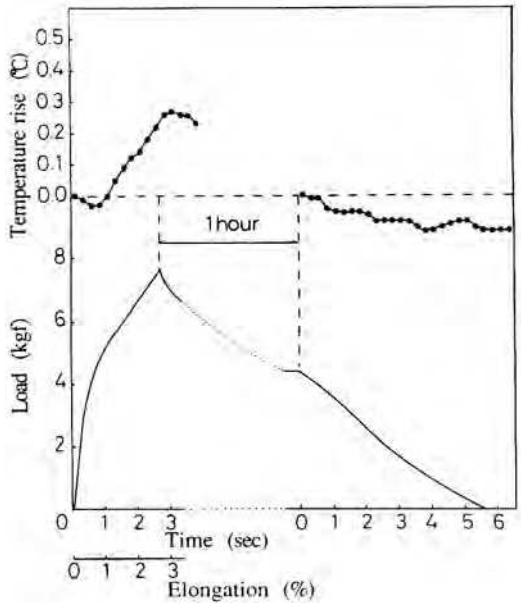


Fig. 7. Changes of load and temperature of paper during tensile straining, stress relaxation, and destraining periods (Yamauchi and Tanaka, 1994).

unexpectedly, the temperature gradually falls, although the extent of the temperature drop is smaller than that of the temperature rise during straining. For comparison, the changes of load and the average temperature of rubber during the same loading and unloading process are shown in Fig. 8. The temperature change indicates typical entropy elasticity, that is, the

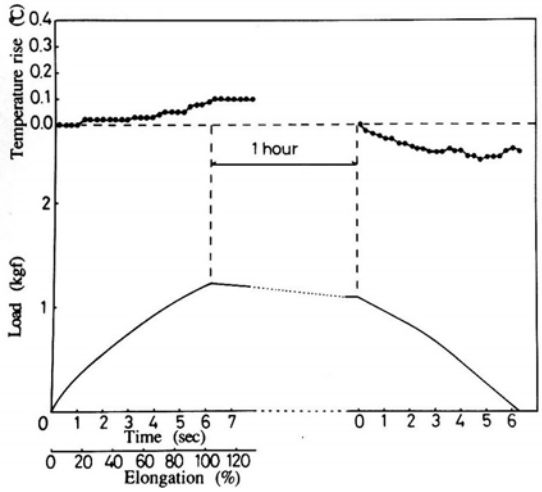


Fig. 8. Changes of load and temperature of rubber during tensile straining, stress relaxation, and destraining periods (Yamauchi and Tanaka, 1994).

temperature increase on straining from the start, and falls on destraining after the stress relaxation period. These results for paper suggest that elastic deformation based on energy elasticity occurred from the beginning of elongation and plastic elongation partly arose from deformation based on entropy elasticity. Further study is expected to clarify the role of entropy elasticity to plastic deformation for various types of paper.

## 6. Effect of paper formation on the deformation pattern shown as thermal images

Successively obtained thermal images of paper on loading (see Fig. 4) included a temperature irregularity arising from the measuring location condition. This is irrelevant in a thermodynamic study based on the change of average temperature; however a discussion of thermal distribution within an image needs a real thermal image and the thus a net thermal image was obtained by image subtraction between chronologically adjacent images, since the dimensional change of paper during that time was negligible (Yamauchi and Murakami, 1992). Paper is a fairly homogenous material and thermal change under loading occurred in fairly uniform manner throughout the specimen up to the moment of breakage (Dumbleton et al., 1973; Yamauchi and Murakami, 1992; 1993) .On the other hand, poorly formed paper, which has heterogeneous mass distribution, showed a marked uneven distribution in the higher temperature region (red part surrounded by yellow part) in the early stage of plastic deformation, but at a later stage of plastic deformation the temperature rise image became homogenous, as shown in Fig. 9 (Yamauchi and Murakami, 1993; 1994). Taking into consideration that paper often starts to break from the low mass region at the edge, more precise serial thermal images and soft X-ray images measured before elongation giving the mass distribution were required, as shown in Fig. 10 (Yamauchi and Murakami, 1994). These images allow us to follow the deformation process in more detail and to find a relationship between the temperature rise distribution and the mass distribution. The final

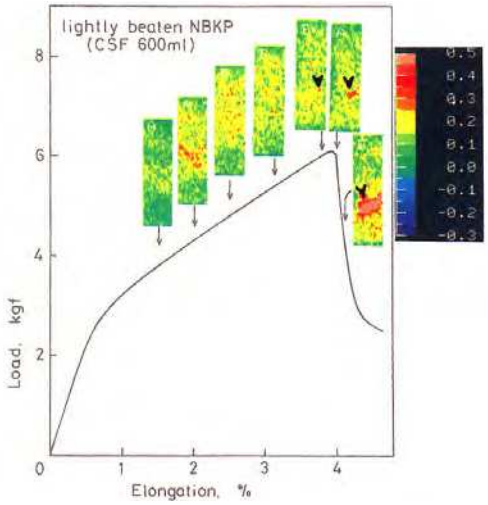


Fig. 9. Load/elongation relation and subtracted temperature rise distribution images during tensile straining of poorly —formed paper (Yamauchi and Murakami, 1994).

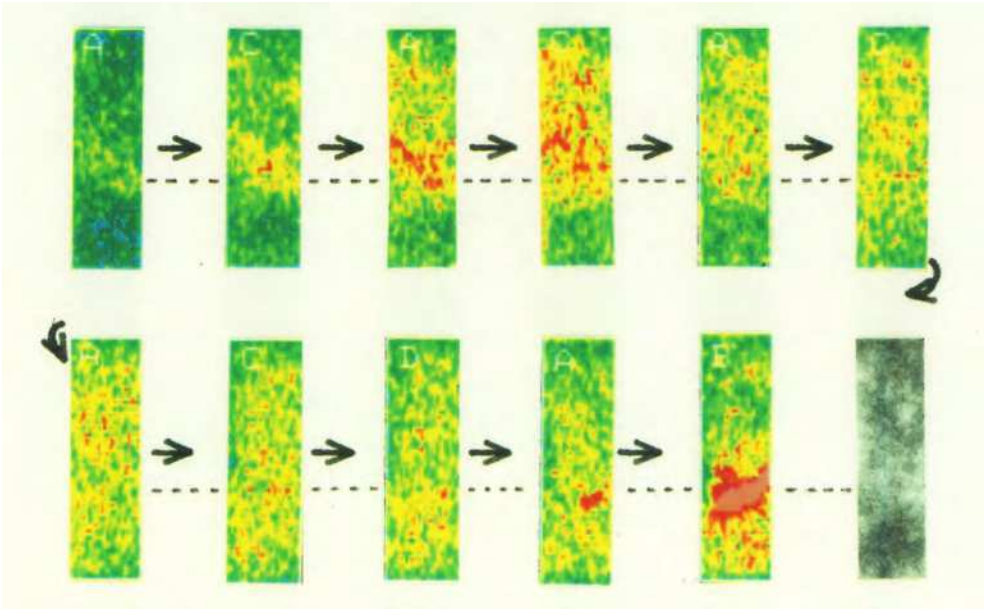

Fig. 10. Sequential subtracted temperature rise distribution images during straining and the soft X-ray mass distribution image of poorly—formed paper (Yamauchi and Murakami, 1994).

failure line marked by black arrows in Fig. 9 did not start from the edge but from a point within the specimen in this case.

Even within the same sample having the same poor formation (mass distribution), the relation between the deformation process, shown as sequential temperature rise distribution images, and breaking load/elongation, somewhat differs in each test. The results of four specimens from the same paper were compared in Fig. 11 with the breaking load, elongation and the soft X-ray image. Case 1 shows the shortened form of Fig. 10. In all these cases except case 4, the final failure line (pink part) started to run from one of the higher temperature regions (red and yellow part) in the early stage of plastic deformation, although these points often became indistinctive in the middle stage of plastic deformation. Thus, the failure-starting point can be predicted in the early stage of plastic deformation. The final failure is interestingly running through the one low mass (thin) part of the specimen, as shown on the soft X-ray image.

Temperature rise distribution images in case 4 were comparatively uniform, i.e., there is no distinctive sign showing the final failure line before breakage. Based on the fact that well—formed paper having uniform mass distribution showed a uniform deformation pattern, shown as uniform images of the temperature rise, and gave a higher breaking load (7.1 kgf), the higher breaking load in case 4 (6.8 kgf) suggested that the extent of uniformity in temperature rise distribution during straining, rather than that in mass distribution, was more directly related to the degree of stress concentration and thus to the breaking load.

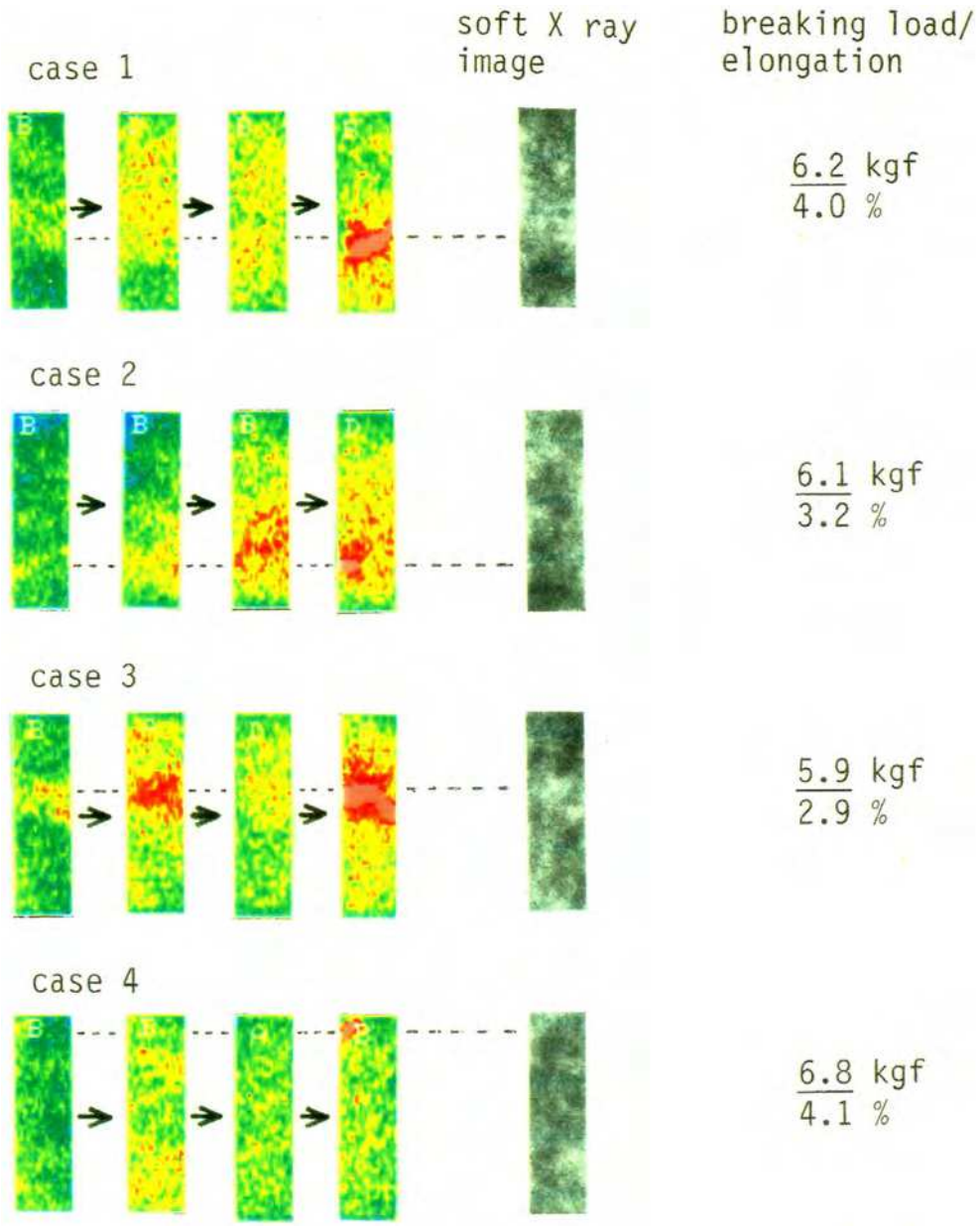


Fig. 11. Variation in the subtracted temperature rise distribution images, mass distribution image and breaking load/elongation of poorly—formed paper (Yamauchi and Murakami, 1994).

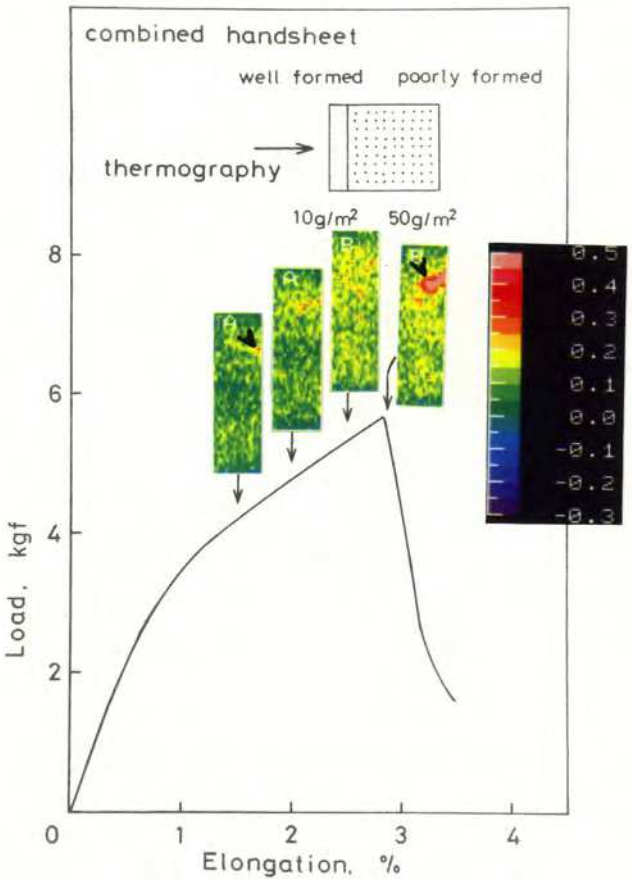


Fig. 12. Load/elongation relation and subtracted temperature rise distribution images during tensile straining of paper composed with well—and poorly—formed layers; the images were observed from the well—formed side.

In order to confirm the assumption that thermal behavior based on the surface temperature of paper is the real thermal behavior of paper itself using the difference derived from the formation in thermal behavior on loading, a special paper combined with well and poorly formed paper layers was prepared and its sequential temperature rise distribution images during tensile straining were observed from the well—formed layer side. Figure 12 shows the result of paper composed of a 10 g/m² well—formed layer and a 50g/m² poorly—formed layer. If the observed sequential temperature rise distribution image is not the thermal behavior of the paper itself but the surface thermal behavior, thermal change under loading should be uniform throughout the specimen up to the moment of breakage. However, uneven distribution of the higher temperature region, which finally developed to the breaking point, was observed at the early stage of plastic deformation. That is to say, the thermal behavior of paper observed as the surface temperature could be assigned to that of the paper itself.

## 7. Application of thermography for studying fracture toughness testing of paper

Relating to the simple elongation testing of paper to determine the tensile strength, fracture toughness testing was conducted using a paper specimen with notch (Niskanen, 1993). The ability of a paper to resist crack propagation from the notch tip under tensile loading is quite important in a number of end-use situations, as well as in papermaking processes. At the manufacturing, printing, and converting operations, stresses are concentrated around the defects in the plane of paper sheet. Thus, in-plane fracture toughness testing has been mainly investigated for paper specimens with center, single or double side notches. During testing, stress is concentrated on around the notch tip and resistance (work) to failure before the start of crack propagation was determined as crack tip opening displacement, J-integral and essential work of fracture (EWF) (Hirano and Yamauchi, 2000). The change in stress distribution, shown as sequential temperature rise distribution, and movement of the crack tip, shown as the shift of the highest temperature point during testing, could be visualized using thermography (Tanaka et al.,1997; Yamauchi and Hirano, 2000). The advantages of thermography are fully used to obtain the sequential changes of thermal images during testing to study the fracture toughness and the testing method itself.

In the measurement of the EWF for fracture toughness developed originally for ductile metals (Cotterell and Reddel, 1977), deep double-edge notched tension (DENT) specimens of various widths were employed as shown in Fig. 13. When a specimen completely yields

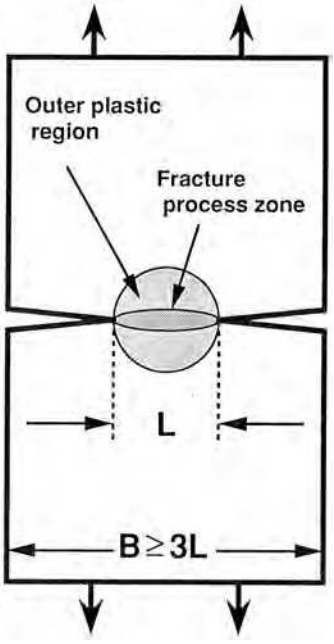


Fig. 13. Deep double-edge notched tension specimen for in-plane fracture toughness testing, showing the fracture process zone and the outer plastic deformation region (Cotterell and Reddel,1977) (B: specimen width, ***L***.: ligament length).

before fracture, a plastic deformation zone is theoretically supposed to be a circular area centered on the ligament (between double notches, one third of the width, displayed in ***L***). Further, the work performed to fracture paper specimen can be separated into two components: (1) the essential work performed in the fracture process zone and (2) the non essential work performed in the plastic deformation zone, and a linear relationship is expected between ***L*** and (specific) work for fracture ($w_f$). In this method the appearance of the circular plastic deformation zone on local process zone before onset of stable crack growth should be a prerequisite for this measurement. Thus, detection of the fracture process zone was tried by both methods, silicone impregnation and thermography (Tanaka et al., 2003), and further development of the plastic deformation zone during testing was examined on sequential close-up temperature rise distribution images, as shown in Fig.14,15. At the moment of fracture during testing, stress is concentrated as expected at the tip of notches, shown as a rise of temperature around the notch tips (I) and no thermal change at the region far from notch tips(II) in Fig. 14. Sequential close-up temperature rise distribution images displayed in more detail the stress concentration and further the appearance of a circular plastic deformation zone from halfway through the plastic deformation region. In practice, the blue spot, whose temperature is higher than the surroundings, firstly appeared around the notch tips (Fig. 15; d,e). These spots spread out toward the inside, and then the enlarged spots joined together just after the maximum load point (Fig. 15; h). Finally, the whole shape of the amalgamated high-temperature zone became circular just before failure (Fig. 15; i). On the other hand, the notch tip has moved

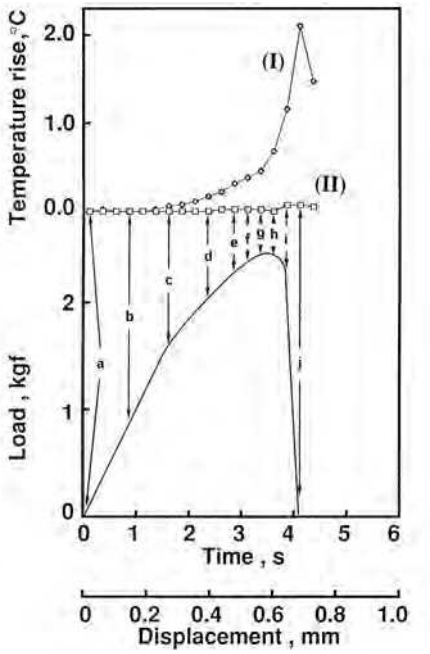


Fig. 14. Changes of the average temperature rise in zone I (around notch tip) and II (far from notch) during testing of paper (handsheet from beaten pulp, ligament: 5mm) and the corresponding load-displacement curve (Tanaka et al., 1997).

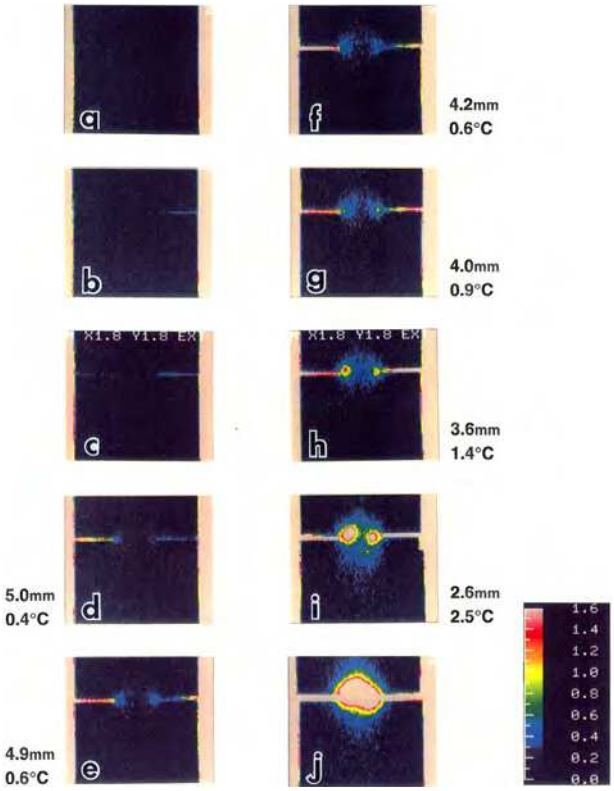


Fig. 15. Sequential close-up temperature rise distribution images of paper (handsheet from beaten pulp, ligament: 5mm); (a)—(j) correspond to the positions on the load-displacement curve in Fig. 8a. Beside each image, the distances between the maximum temperature points around both notch tips are shown with the temperature rise (Tanaka et al., 1997).

toward the inside even before the stage of maximum load, as shown by a decrease in the distance between the maximum temperature points (Fig. 15; e,f,g) This movement means stable crack growth, and further onset of crack growth before maximum load point to sheet failure was confirmed by means of direct observation of the notch tip using video-microscopy (Tanaka and Yamauchi, 1999).

As the theoretical prerequisite for EWF, the development of a circular plastic deformation zone in the ligament before crack growth is required. Thus, sequential close-up temperature rise distribution images were examined for specimens of various ligament lengths (Tanaka and Yamauchi, 2000) and further the plastic deformation zone was theoretically estimated (Tanaka and Yamauchi, 1997). As a result, the plastic deformation zone appears in three ways: 1. Type (i) appearing through the whole ligament in a vague manner and developing into a circular (or oval) zone even before or at the maximum load point; (see Fig. 16 and 17 for UKP-sack paper in cross direction loading: CD); 2. Type (ii) appearing from the notch tip and amalgamating into a circular (or oval) zone after the maximum load point (see Fig. 18 and 19 for UKP-sack paper in CD loading); and 3. Type (iii) appearing from the notch tip

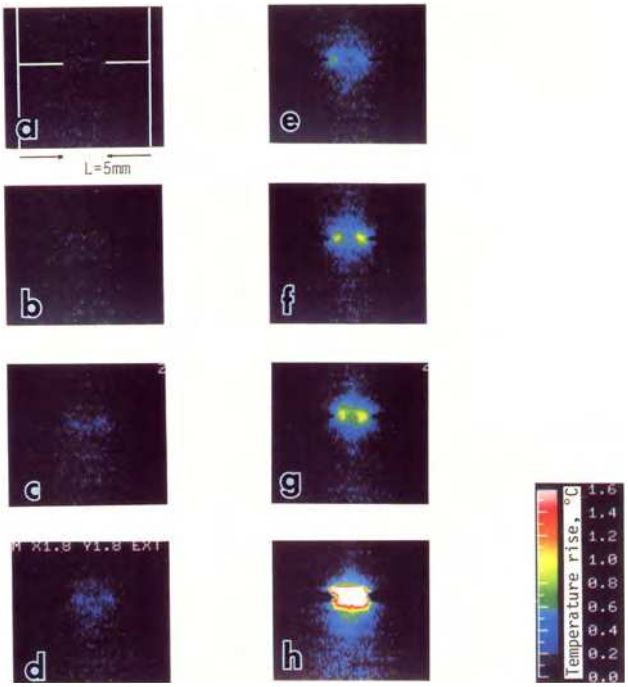


Fig. 16. A series of close-up temperature rise distribution images of UKP-sack paper (CD/***L***: 5mm); (a)—(h) correspond to the positions on the load-displacement curve in Fig.17 (Tanaka and Yamauchi, 2000).

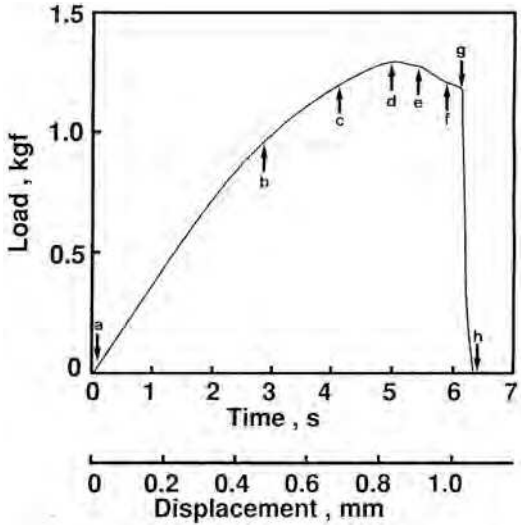


Fig. 17. Load-displacement curve for the UKP-sack paper (CD/***L***: 5mm) (Tanaka and Yamauchi, 2000).

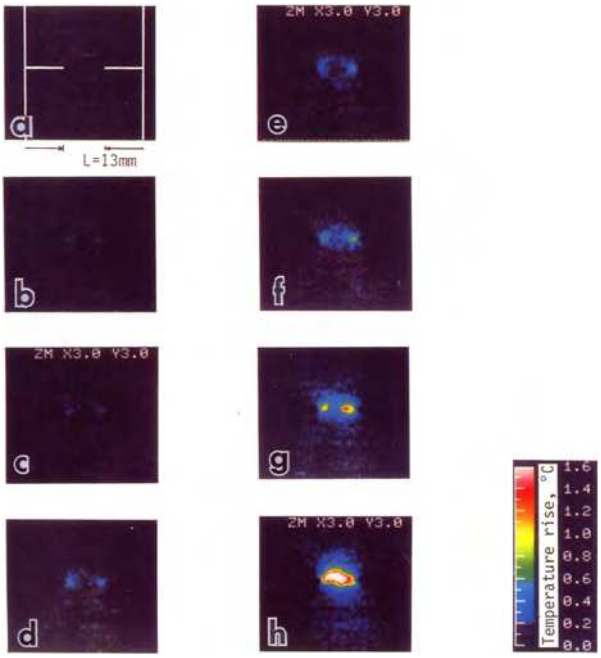


Fig. 18. A series of close-up temperature rise distribution images of UKP-sack paper (CD/***L***: 13mm); (a)—(h) correspond to the positions on the load-displacement curve in Fig. 19 (Tanaka and Yamauchi, 2000).

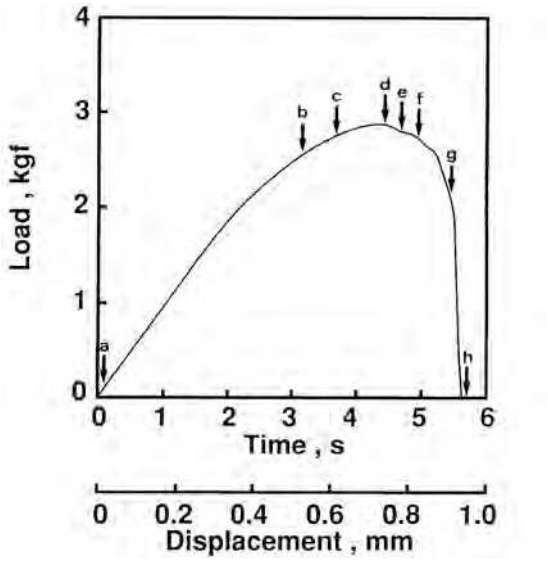


Fig. 19. Load-displacement curve for the UKP-sack paper (CD/***L***: 13mm) (Tanaka and Yamauchi, 2000).

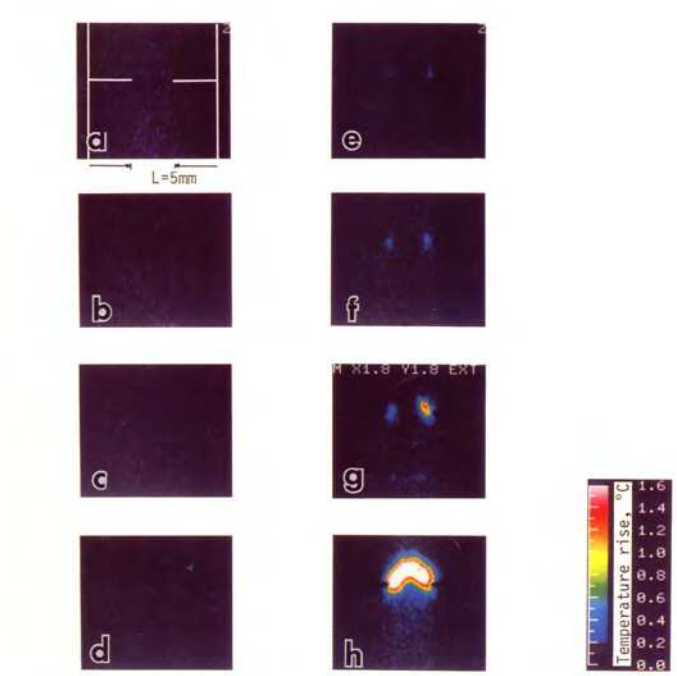


Fig. 20. A series of close-up temperature rise distribution images of UKP-sack paper (MD/***L***: 5mm); (a)—(h) correspond to the positions on the load-displacement curve in Fig. 21 (Tanaka and Yamauchi, 2000).

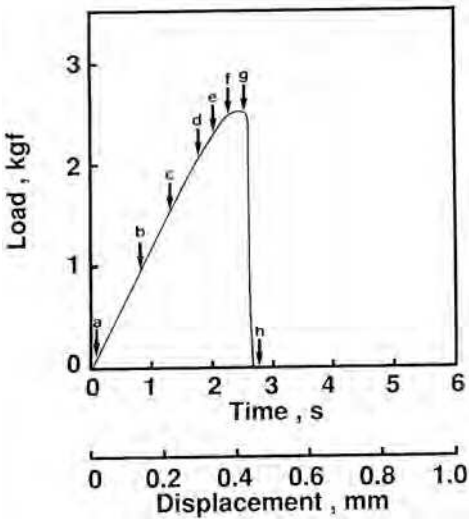


Fig. 21. Load-displacement curve for the UKP-sack paper (MD/***L***: 5mm) (Tanaka and Yamauchi, 2000).

and not amalgamating into a circular (or oval) zone until sheet failure (see Fig. 20 and 21 for UKP-sack paper in machine direction loading: MD). Table 1 shows the type of plastic deformation zone appearance for representative commercial papers of various specimen widths. Paper specimens with a small ligament length (***L***) are likely to belong to type (i), while those with a large ***L*** to type (ii) and (iii). Among these three types, type (i) fulfills the original assumption of the EWF method best in terms of complete ligament yielding before crack initiation. Thus, the specific EWF determined by using the extrapolation of the linear relation of type (i) to ***L***=0 should be correct, although the estimated work (EWF) is a little smaller than that from the linear relation of type (ii) and (iii) without exception, as shown in Fig. 22. Furthermore, the corrected experimental plots based on theoretical calculation for large ligament specimens had almost the same linear relation as small ligament specimens, as shown in Fig. 23 (The scale of ordinate spread to three times. Tanaka et al., 1998).

| | | L=1mm | L=2mm | L=3mm | L=4mm | L=5mm | L=9mm | L=13mm | L=17mm | L=21mm |
|---|---|---|---|---|---|---|---|---|---|---|
| UKP -sack | MD | (i) | (i) | (ii) | (iii) | (iii) | (iii) | (iii) | (iii) | (iii) |
| | CD | (i) | (i) | (i) | (i) | (i) | (ii) | (ii) | (ii) | (ii) |
| Machine grazed | MD | (i) | (i) | (i) | (ii) | (iii) | (iii) | (iii) | (iii) | (iii) |
| | CD | (i) | (i) | (i) | (i) | (ii) | (ii) | (ii) | (ii) | (ii) |
| News print | MD | (i) | (i) | (ii) | (iii) | (iii) | (iii) | (iii) | (iii) | (iii) |
| | CD | (i) | (i) | (i) | (i) | (ii) | (iii) | (iii) | (iii) | (iii) |
| Filter | MD | (i) | (i) | (i) | (i) | (ii) | (iii) | (iii) | (iii) | (iii) |
| | CD | (i) | (i) | (i) | (i) | (i) | (ii) | (iii) | (iii) | (iii) |

Table 1. Type of plastic deformation zone appearance for representative commercial paper specimens of various specimen widths (***L***=1/3 width)

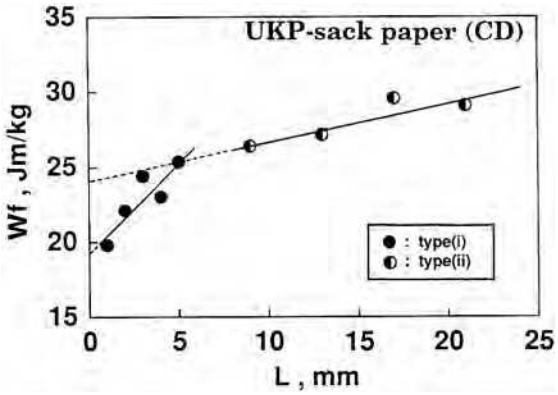


Fig. 22. Experimental determination of the specific essential work of fracture by extrapolation of the linear relation between work of fracture ($w_f$) and ligament length (***L***) for UKP-sack paper (CD) (Tanaka and Yamauchi, 2000).

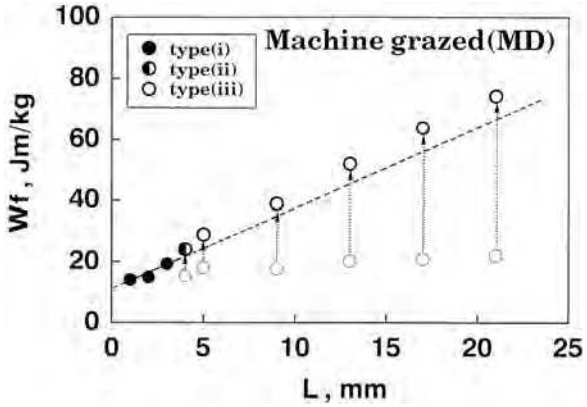


Fig. 23. Corrected experimental plots between work of fracture and ligament lengths for machine grazed paper (MD). Broken arrows show corrections (The scale of ordinate spread to three times Tanaka et al., 1998).

For in-plane fracture toughness testing, J-integral and crack tip opening displacement other than EWF have also been introduced for paper materials. The thermal images during these testing gave much knowledge on the examination of these methods (Hirano and Yamauchi, 2000). Further, the sequential thermal images gave some suggestions for studying the effects of notch application and its geometry (Yamauchi, 2004).

## 8. Application of thermography to tearing test of paper

As described above, fracture toughness is estimated as the work required to fracture a notched specimen, and the fracturing of planar materials including paper has two modes, in-plane and out-of-plane. In the former mode, stresses are applied along the plane of the paper sheet. On the other hand, stress is applied perpendicular to the plane of the paper sheet in the latter mode, which is identical to out-of-plane tearing, known as Elmendorf tearing. Compared with in-plane and out-of-plane tearing, the cumulative energy of the micro failures that occurred during out-of-plane tearing was markedly larger than that during in-plane tearing, as shown in thermal distribution images on tearing (Yamauchi, 2005). The development of stress concentration at the notch tip was observed as close-up sequential thermal distribution images and 3-D images of temperature rise on tearing, as shown in Fig. 24 (Tanaka and Yamauchi, 2005). The size of the area where heat was generated during tearing decreased, i.e. the degree of stress concentration increased with an increase of the beating degree for a paper sheet made from longer fibers. The ratio of heat generation to tearing work was ~10%, which is smaller than the corresponding ratio of 40 to 80 % for tensile testing (referring to the end of first paragraph of **3**. Temperature (heat) change, see Fig. 6). Furthermore, heat generation was classified as that attributable to damage and plastic deformation. In order to evaluate heat generation caused by damage (fiber pull out and breakage) around the crack tip, a threshold Tb showing the end of plastic deformation (yielding) and onset of damage was applied to the above 3D-image of temperature rise on tearing. Although some damage occurred slightly before paper breakage at maximum loading, most of the damage occurred at or after the maximum load

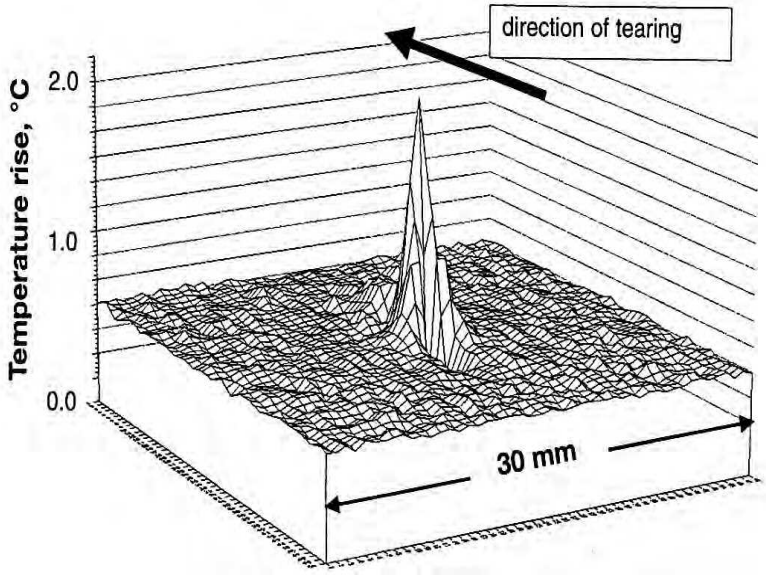


Fig. 24. 3D-image of temperature rise on tearing. obtained by image subtraction of handsheet from beaten pulp (Tanaka and Yamauchi, 2005).

point (Tanaka and Yamauchi ,1999). The schematic image of such thresholds is shown in Fig. 25. The tearing energy of paper from long—fibered pulp correlates well with heat from the damage.

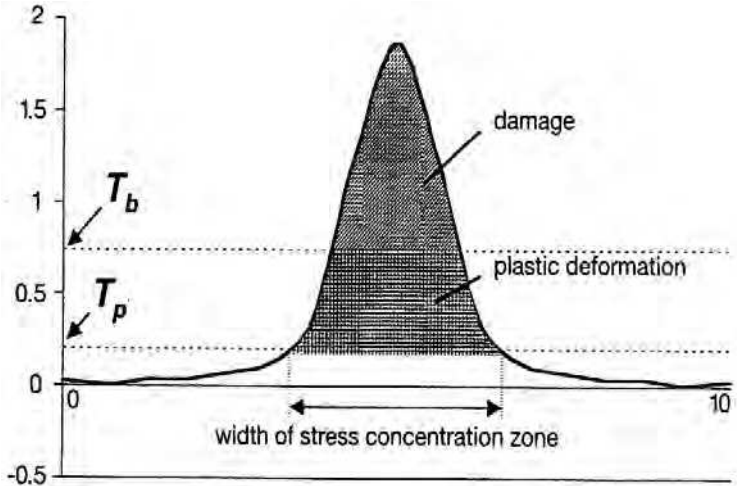


Fig. 25. Schematic image of threshold temperature. The curve shows the cross section of the 3-D image. Tp: threshold for plastic deformation and Tb: threshold for damage (fiber pull out or breakage) (Tanaka and Yamauchi, 2005).

## 9. Subsequent studies on paper materials using thermography

Thermography is applicable to identify hidden air-filled defects within the thickness of laminated paperboard (Sato and Hutchings, 2010). In a thermally non-stationary state, the region over a defect can be visually distinguished from neighboring defect-free areas by its thermal contrast. For quantitative determination, the pulsed thermography method was used and temperature history curves were examined in order to characterize the unknown defects. It was found that a defect can be quantitatively evaluated in a reasonable time at a depth of less than 2mm beneath the surface. Compared with many other materials, paper has higher specific heat and lower thermal conductivity, and thus the thermal contrast persists for a longer time.

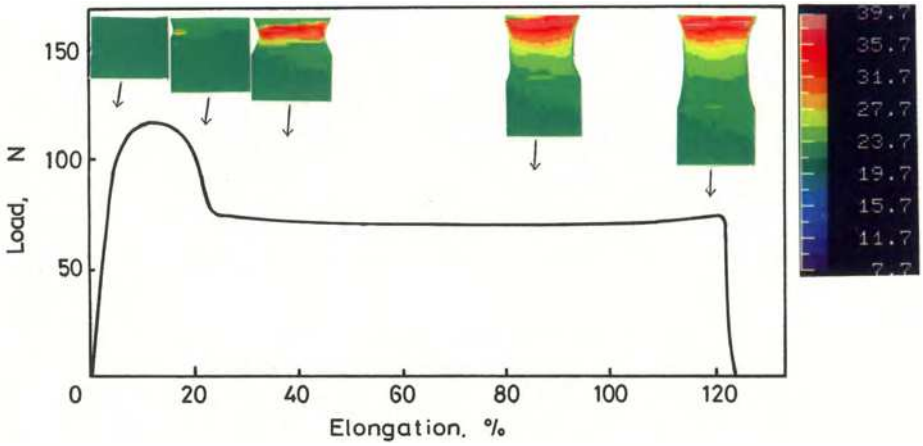


Fig. 26. Relationship of load-elongation, and some selected temperature distribution images of drawn PP film (Yamauchi, 2006).

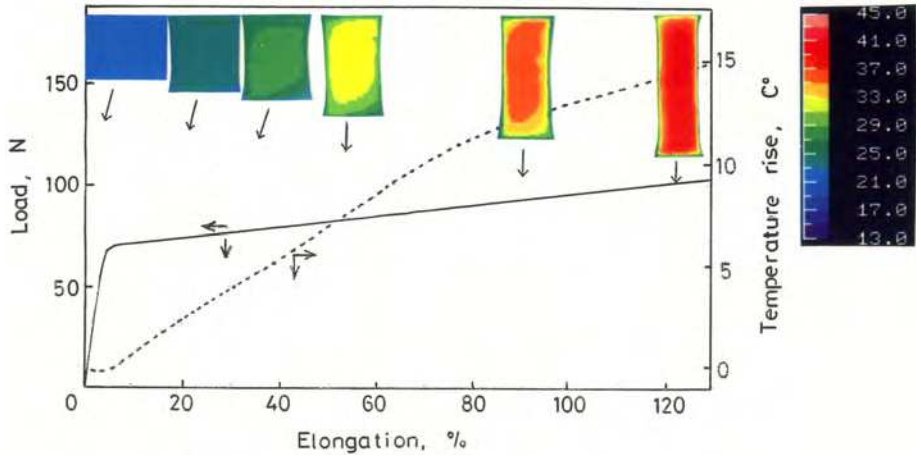


Fig. 27. Relationships of load and temperature rise—elongation, and some selected temperature distribution images of drawn PET film.

Additionally, heat generation that accompanied tensile drawing for other planar material, polymer film, was successfully observed using thermography (Yamauchi, 2006). The sequential temperature rise distribution images showed that the high temperature region, where rearrangements of molecular orientation and microcrystallines occurred, was located mainly at the upper end of the necked part for films that exhibited necking as shown in Fig. 26, or appeared uniformly throughout films for the polymers that did not exhibit necking behavior as shown in Fig.27.

## 10. Summary

Study on deformation and fracture of paper is very important as a fundamental of its strength properties. Thermal behavior with its deformation and fracture as shown in chronologically sequential surface temperature images can be successfully investigated by using IR thermography, since paper is a two-dimensional planar material and its thermal conductivity is low and further its specific heat is high. As the thermodynamics of paper deformation, heat absorption caused by Kelvin's thermoelastic effect at the elastic deformation region and heat generation in the plastic deformation region were observed, and further suggested that elastic deformation based on energy elasticity occurred from the beginning of elongation and plastic elongation partly arose from deformation based on entropy elasticity. Paper is a fairly homogenous material as shown in uniform planar mass distribution and its thermal change under loading occurred in fairly uniform manner throughout the specimen up to the moment of its breakage. On the other hand, poorly formed paper, which has heterogeneous mass distribution, showed an uneven distribution in the higher temperature region at the early stage of plastic deformation, but at a later stage of plastic deformation the temperature image became homogenous. The extent of uniformity in temperature rise distribution during straining, rather than that in mass distribution, was more directly related to the degree of stress concentration within the specimen and thus to the breaking load of paper. On essential work of fracture (EWF) toughness testing as a one of the in-plane fracture toughness testing, the stress concentration around the tip of notches and the appearance of a circular plastic deformation zone centered on the ligament (between double notches, one third of the width) from halfway through the plastic deformation region could be visualized using thermography as sequential temperature rise distribution images, and further movement of the crack was shown as the shift of the highest temperature point during testing. Paper specimens with a small ligament fulfilled the original assumption of the EWF method best in terms of complete ligament yielding before crack initiation. Thus, the specific EWF determined by using the extrapolation of the linear relation between ligament and work of fracture for the specimens with a small ligament should be correct, although the estimated EFW is a little smaller than that for the specimen with bigger ligament. Thermal distribution images on paper tearing showed that the cumulative energy of micro failures that occurred during out-of-plane tearing was markedly larger than that during in-plane tearing. The size of the area where heat was generated during tearing decreased, i.e. the degree of stress concentration increased with an increase of pulp beating for a paper sheet made from longer fibers. The tearing energy of paper from long-fibered pulp correlates well with heat from the fiber pull out and breakage around the crack tip. Thermography is a unique and versatile technology, and thus applicable to study on water absorption and moisture profile of paper, except for study on its deformation and fracture as described above.

## 11. Acknowledgement

The author expresses his huge thanks to co-worker, Dr Atsushi Tanaka (presently VTT Finland), and to the Laboratory of Wood Processing in the Graduate School of Agriculture, Kyoto University for permission to use the thermogrphy system, and also thanks to Arakawa chemical, Rengo and Showa products Co. Ltds for their financial support.

## 12. References

Chao, Y.J. and Sutton, M.A. (1988). Measurement of strains in a paper tensile specimen using computer vision and digital image correlation Part 2:Tensile specimen test. *Tappi J.*,Vol. 71, No.4, pp.153-156

Cotterell, B. and Reddel; J.K. (1977). The essential work of plane stress ductile fracture. *Int. J. Fracture*, Vol. 13, pp. 267-277

Dumbleton, D.P., Kringstad, K.P. and Soremark, C. (1973). Temperature profiles in paper during straining. *Svensk Papperstid,* Vol.76, No.14. PP.521-528

Ebeling, K.I, Swanson, J.W. and Van den Akker, J.A. (1974). Microcalorimeter for measuring heat of straining or destraining of sheet-like materials. *Rev. Sci. Instrum.*, Vol.45, No.3. pp. 419-426

Ebeling, K.I. (1976).Distribution of energy consumption during the straining of paper, In *The fundamental properties of paper related to its uses,* F. Bolam(ed), pp.304-343

Hirano, H. and Yamauchi; T. (2000). J-integral Jc and crack tip opening displacement CTODc as a material property evaluating the fracture toughness of paper. *J. Tappi Jpn.*,Vol.54, No.5, pp 75-80

Koizumi, T. (1983) .On thermo-elasticity measurement. *NDT Jpn*., Vol.32, No.7, pp.61-565

Muller, F.H. (1969). Thermodynamics of deformation: Calorimetric investigations of deformation processes, In *Rheology, Theory and Application* Vol.5 , F.R. Eirich (Ed), pp.417-489, Academic Press

Niskanen, K. (1993). Strength and Fracture of paper, In *Products of Papermaking*, C.F. Baker (Ed) pp.641-725

Reifsnider, K.L. and Williams, R.S. (1974). Determination of fatigue-related heat emission in composite materials. *Experimental Mechanics*, Vol.14, pp.479-485

Sato, J. and Hutchings, I.M. (2010).Non-destructive testing of laminated paper products by active infra-red thermography. *Appita J.*, Vol.63, No.5, pp. 399-406

Seth, R.S. and Page, D.H. (1981). The stress-strain curve of paper, In *The Role of Fundamental Research in Paper Makin,g* F. Bolam (Ed), pp. 421-452

Tajima, T., Ueno, S., Yabu, N. and Sukigara, S. (2011) Fabrication and characterization of Poly-$\gamma$-glutamic acid nanofiber with the difunctional epoxy cross-linker. *Seni' Gakkaishi* , Vol.67, No.8, pp. 169-175

Tanaka, A., Othuka, Y. and Yamauchi, T. (1997). Observation of in-plane fracture toughness testing of paper by use of thermography. *Tappi J.*, Vol.80, No.5, pp. 222-226

Tanaka, A. and Yamauchi, T. (1997). Size estimation of plastic deformation zone at the crack tip of paper under fracture toughness testing. *J. Pack Sci .& Tech. Jpn.,* Vol.6, No.5, pp. 268-276

Tanaka, A., Matsumoto, T. and Yamauchi, T. (1998). Calculative correction of the essential work of fracture method for paper. *Seni' Gakkaishi* , Vol.54, No.12, pp. 134-140

Tanaka, A. and Yamauchi, T. (1999). Measurement of crack tip opening displacement of paper using CCD camera. *J. Pack Sci. &Tech. Jpn.,* Vol.8, No.1, PP. 11-18

Tanaka, A. and Yamauchi, T. (2000). Deformation and fracture of paper during the in-plane fracture toughness testing —Estimation of the essential work of fracture method—. *J. Materials Sci*., Vol.35, No.7, PP. 1827-1833

Tanaka, A., Kettunen, H. and Yamauchi, T. (2003). Comparison of thermal maps with damage revealed by silicone impregnation. *Paperi ja Puu,* Vol.85, No.5, pp.287-290

Tanaka, A. and Yamauchi, T. (2005). A thermographic observation of out-of- plane tearing process of paper. *Appita J.,* Vol.58, No.3, PP. 186-189. 217

Vickery, D. E., Luce, J.E., and Atkins, J.W. (1978). Infrared thermography An aid to solving paper machine moisture profile problems. *Tappi* Vol.61, No.12, pp.17-22

Yamauchi, T., Okumura, S. and Noguchi, M. (1990). Acoustic emission as an Aid for investigating the deformation and fracture of paper. *J. Pulp Paper Sci.,* Vol.16, No.2, pp.44-47

Yamauchi, T. and Murakami, K. (1992). Observation of deforming and fracturing processes of paper by using infrared thermography. *J. Tappi Jpn*., Vol.46, No.4, pp. 178-183

Yamauchi, T., Okumura, S. and Noguchi, M. (1993). Application of thermography to the deforming process of paper materials. *J. Materials Sci*., Vol.28, No.17, PP. 4549-4552

Yamauchi, T. and Murakami, K. (1993). Observation of the deforming and fracturing processes of paper using thermography, In *Products of Papermaking*, C.F. Baker, (Ed.), pp. 825-847

Yamauchi, T. and Tanaka, A. (1994). Experimental detection of entropy elasticity occurred during the plastic deformation of paper. *J. Applied Polymer Sci*., Vol. 53, No.8. pp. 1125-1127

Yamauchi, T. and Murakami, K. (1994). Observation of deforming process of poorly formed paper sheet by use of thermography. *Seni Gakkkaishi* , Vol.50, No.9, PP.424-425

Yamauchi, T and Hirano, H. (2000). Examination of the onset of stable crack growth under fracture toughness testing of paper. *J. Wood Sci*., Vol.46, pp. 79-85

Yamauchi, T. (2004). Effect of notches on micro failures during tensile straining of paper. *J. Tappi Jpn.,* Vol.58, No.11, pp. 1599-1606

Yamauchi, T. (2005). Differences between in-plane and out-of-plane tensile fracturing of notched paper. *J. Pack Sci. & Tech. Jpn.,* Vol.14, No.5, PP. 329-340

Yamauchi, T. (2006). Observation of polymer film drawing by use of thermography. An introductory investigation on the thermodynamics. *J. Applied Polymer Sci.,*. Vol.100, pp. 2895-2900

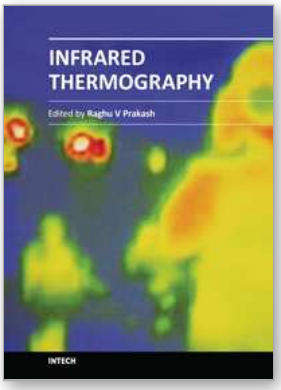


**Infrared Thermography**

Edited by Dr. Raghu V Prakash

ISBN 978-953-51-0242-7
Hard cover, 236 pages
**Publisher** InTech
**Published online** 14, March, 2012
**Published in print edition** March, 2012

Infrared Thermography (IRT) is commonly as a NDE tool to identify damages and provide remedial action. The fields of application are vast, such as, materials science, life sciences and applied engineering. This book offers a collection of ten chapters with three major sections - relating to application of infrared thermography to study problems in materials science, agriculture, veterinary and sports fields as well as in engineering applications. Both mathematical modeling and experimental aspects of IRT are evenly discussed in this book. It is our sincere hope that the book meets the requirements of researchers in the domain and inspires more researchers to study IRT.

**How to reference**

In order to correctly reference this scholarly work, feel free to copy and paste the following:

Tatsuo Yamauchi (2012). Application of IR Thermography for Studying Deformation and Fracture of Paper, Infrared Thermography, Dr. Raghu V Prakash (Ed.), ISBN: 978-953-51-0242-7, InTech, Available from: http://www.intechopen.com/books/infrared-thermography/application-of-ir-thermography-for-studying-deformation-and-fracture-of-paper

INTECH
open science | open minds

**InTech Europe**
University Campus STeP Ri
Slavka Krautzeka 83/A
51000 Rijeka, Croatia
Phone: +385 (51) 770 447
Fax: +385 (51) 686 166
www.intechopen.com

**InTech China**
Unit 405, Office Block, Hotel Equatorial Shanghai
No.65, Yan An Road (West), Shanghai, 200040, China
中国上海市延安西路65号上海国际贵都大饭店办公楼405单元
Phone: +86-21-62489820
Fax: +86-21-62489821